PHYSICAL REVIEW B **81**, 081403(R) (2010)

# Quantum valley Hall effect in proximity-induced superconducting graphene: An experimental window for deconfined quantum criticality

Pouyan Ghaemi,[1] Shinsei Ryu,[1] and Dung-Hai Lee[1,2]
[1]*Department of Physics, University of California–Berkeley, Berkeley, California 94720, USA*
[2]*Material Science Division, Lawrence Berkeley National Laboratory, Berkeley, California 94720, USA*
(Received 30 December 2009; published 4 February 2010)

We show that when superconductivity is induced in graphene through proximity effect, a superconducting vortex is dressed with an interesting pattern of textured order parameters. Furthermore, passing a supercurrent in a superconducting graphene sample induces accumulation of valley pseudospin quantum number at edges: the "quantum valley Hall effect" will be observable in superconducting graphene. These effects reveal a quantum duality between different order parameters that is at heart of the Wess-Zumino-Witten term.

DOI: 10.1103/PhysRevB.81.081403 PACS number(s): 73.20.Mf, 71.10.Fd, 71.23.An, 73.43.Lp

Neutral graphene is a semimetal with two Fermi points ($\mathbf{K}_+$ and $\mathbf{K}_-$) at the Brillouin-zone corners.[1,2] Due to the vanishing density of states and low dimensionality, neutral graphene is quite robust against developing orders. Nevertheless we can force an order to be induced in graphene by proximity to an external symmetry-breaking source. In particular, it has been demonstrated that through a contact with superconducting (SC) electrodes it is possible to send dissipationless current through graphene[3,4]—an experiment which is suggestive of the possibility to induce superconductivity in graphene through the proximity effect[5] (Fig. 1).

It turns out that if this is achieved, the vortex core of SC graphene will have two mid gap states, one for each valley $\mathbf{K}_\pm$.[6] These states can be viewed as a spin-1/2 pseudospin degree of freedom ("valley pseudospin") by regarding two valleys $\mathbf{K}_\pm$ as "spin up" and "spin down," respectively. The purpose of this Rapid Communication is to show the valley pseudospin accumulated at a vortex core leads to a number of interesting observable consequences in SC graphene. In particular, it makes the core acquire a texture of the Kekule type bond or charge-density wave (CDW) orders. Furthermore, this is related to, as we will see, yet another interesting phenomena: the quantum valley Hall effect (QVHE).

The mechanism behind the order-parameter texture of the vortex core is as follows: in reality two mid gap states are not exactly degenerate and the pseudo spin rotation symmetry is broken. (One source of symmetry breaking is the inhomogeneity caused by the vortex itself, which causes scattering between $\mathbf{K}_\pm$.) Such symmetry breaking can be represented by a pseudo magnetic field $\boldsymbol{B}_{\text{eff}}$ acting on the pseudospin 1/2 in-gap states. If $\boldsymbol{B}_{\text{eff}}$ points in the $z$ direction the resulting split states exhibit CDW order (see Fig. 3). On the other hand if $\boldsymbol{B}_{\text{eff}}$ lies on the $xy$ plane a valence bond type order—the Kekule order results are exhibited (see Fig. 2).

Even in the presence of the symmetry breaking the pseudospin component along the $\boldsymbol{B}_{\text{eff}}$ direction is still a good quantum number. Consequently there is an conserved pseudospin current associated with it. We will show that a time-dependent supercurrent induces this pseudospin current, very much like the electric field induces a spin current in the quantum spin Hall effect.[7,8] As a result, if we ramp the supercurrent from zero to some fixed value, an accumulation of the pseudospin polarization will result. Again, depending on the direction of symmetry breaking $\boldsymbol{B}_{\text{eff}}$, this can correspond to a shift in the CDW or the Kekule pattern (Fig. 4).

We will show that all of the above phenomena, vortex core accompanying an order-parameter texture and the QVHE, can be described in an unifying way by the "double Chern-Simons" action given in Eq. (3). The physics underlying the QVHE is the same to that of a type of quantum phase transition, namely, the "deconfined quantum criticality"[9]—a continuous phase transition connecting two quantum phases with unrelated symmetries. What makes it possible is the fact that the defects of one ordered phase carry the quantum number of the order parameter of the other phase [e.g., the dislocation of the valence bond solid (VBS) carries spin whose long-range-order results in the Neel state]. The situation here in SC graphene is quite analogous: a vortex (the defect of the SC order) carries the pseudospin quantum number—the quantum number of the CDW or Kekule order parameter. Thus observing the vortex core structure predicted here provides an experimental window for peeking at the working principle of deconfined quantum criticality. We should stress, however, that we are not predicting that deconfined quantum criticality will occur in proximity-induced superconducting graphene, since in our setup vortices are created externally and are not dynamical.

The physical system we consider consists of a bulk type II $s$-wave superconductor coated by a single layer graphene (Fig. 1). When electron tunneling between the superconductor and graphene layer is sufficiently strong, superconductivity can be induced, through the proximity effect.[5] In

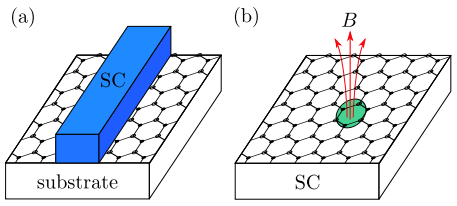


FIG. 1. (Color online) Two setups for proximity-induced superconductivity and the quantum valley Hall effect in graphene. (a) A superconducting electrode is placed on graphene. (b) A superconducting vortex is introduced together with small staggered potential (shaded region) near the core, which allows detection of accumulated valley spin.

 

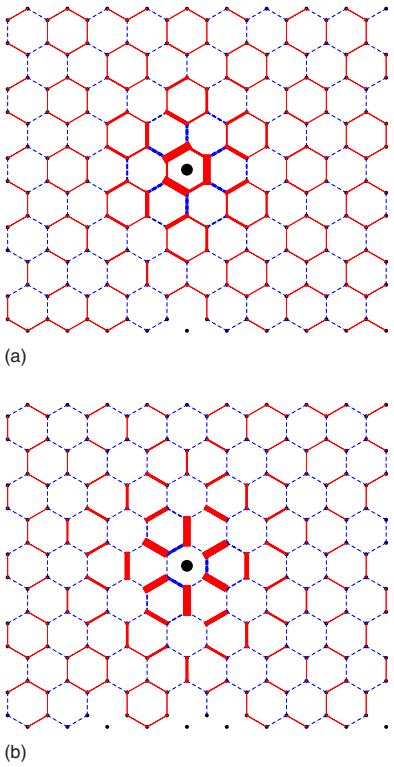


FIG. 2. (Color online) Kekule texture observed for the split core states at (a) positive and (b) negative energy. Dotted (blue)/solid (red) lines show strengthened/weakened bonds, respectively. The filled circle denotes the position of the vortex.

the following we consider the simplest case where graphene becomes a *s*-wave superconductor through proximity effect. The Bogoliubov de Gennes (BdG) Hamiltonian is given by $\mathcal{H}=\int d\mathbf{r}\Psi^{\dagger}K\Psi$, where

$$K=\begin{pmatrix} h & \Delta\Lambda \\ \Delta^{*}\Lambda^{-1} & -h^{T} \end{pmatrix}, \quad \Psi=\begin{pmatrix} \psi_{\uparrow} \\ \psi_{\downarrow}^{\dagger T} \end{pmatrix}. \tag{1}$$

Here $\psi_s=(\psi_{A+s},\psi_{B+s},\psi_{A-s},\psi_{B-s})^T$ is the four component fermionic field. $\psi_{A/B,+/-,s}$ represents the electron annihilation operator on sublattice $A/B$ associated with valley $\mathbf{K}_{\pm}$ and spin $s$. In the following, we use three sets of Pauli matrices, $\{\tau_{x,y,z,0}\}$, $\{\sigma_{x,y,z,0}\}$, and $\{\rho_{x,y,z,0}\}$, each acting on sublattice $(A,B)$, valley $(+,-)$ and Nambu $(\psi_{\uparrow},\psi_{\downarrow}^{\dagger T})$ degrees of freedom, respectively (the displayed $2\times2$ structure in Eq. (1) is associated with the Nambu degrees of freedom). In Eq. (1), $h$ is given by $h=\mathrm{diag}(h_{+},h_{-})$ where $h_{\pm}\equiv-i(\tau_x\partial_x\pm\tau_y\partial_y)$, with the Fermi velocity set to one for convenience; the term $\Delta\Lambda$ with $\Delta\in\mathbb{C}$ and $\Lambda=\sigma_x\tau_z$, pairs electrons associated with $\mathbf{K}_{+}$ and $\mathbf{K}_{-}$.

For the two degenerate valleys one can introduce the pseudospin operators as $\mathcal{Q}_i:=(1/2)\int d\mathbf{r}\Psi^{\dagger}Q_i\Psi$, where $(Q_1,Q_2,Q_3)=(\tau_x\sigma_y\rho_0,-\tau_x\sigma_x\rho_z,\tau_0\sigma_z\rho_z)$. They satisfy $[Q_i,Q_j]=2i\epsilon_{ijk}Q_k$. One can check pseudospin is conserved since $Q_i$ commutes with the BdG Hamiltonian $K$.

Now we examine the core structure of a SC vortex in SC graphene. The vortex is created by applying magnetic field perpendicular to the graphene plane, which induces vortex lines in the bulk superconductor and pass through the graphene layer. With a single vortex (with vorticity $n$) centered at $\mathbf{r}=0$ the $\Delta$ in Eq. (1) becomes $\Delta(|\mathbf{r}|)e^{in\theta}$ where $\Delta(|\mathbf{r}|)\propto|\mathbf{r}|^n$ as $|\mathbf{r}|\to0$ and $\Delta(|\mathbf{r}|)\to\Delta$ as $|\mathbf{r}|\to\infty$. In addition the magnetic field is introduced via the vector potential through minimal coupling. In the presence of the vortex the BdG equation $K\Psi(\mathbf{r})=E\Psi(\mathbf{r})$ acquires two zero energy solutions if the vortex profile is sufficiently smooth so that it does not cause single-particle scattering between $\mathbf{K}_{+}$ and $\mathbf{K}_{-}$ (for simplicity we consider a single winding vortex).[6] In the symmetric gauge $\mathbf{A}(\mathbf{r})=A(|\mathbf{r}|)\mathbf{e}_{\theta}$, the zero energy eigenfunctions $\Psi_1(\mathbf{r})$ and $\Psi_2(\mathbf{r})$ are given by

$$\Psi_1^T(\mathbf{r})=[f(|\mathbf{r}|),0,0,0,0,0,0,-if(|\mathbf{r}|)],$$

$$\Psi_2^T(\mathbf{r})=[0,0,0,-if(|\mathbf{r}|),f(|\mathbf{r}|),0,0,0], \tag{2}$$

where the localized function $f(|\mathbf{r}|)$ is given by $f(|\mathbf{r}|)=e^{q\int_0^{|\mathbf{r}|}A(s)ds}g(|\mathbf{r}|)$ with $g(|\mathbf{r}|)\to$constant $(|\mathbf{r}|\to0)$ and $g(|\mathbf{r}|)\to e^{-\Delta|\mathbf{r}|}$ $(|\mathbf{r}|\to\infty)$ $(q>0$ is the electric charge). While our results here are presented for half filling (zero chemical potential), zero modes continue to exist for finite doping.[10]

Interestingly the two degenerate vortex core states form a spin-1/2 representation of the pseudospin operators $\mathcal{Q}_i$, so that within the two-dimensional space of the midgap states $\mathcal{Q}_i$ is represented by a $2\times2$ Pauli matrix $\Gamma_i$. The wave function given by Eq. (2) are eigenvectors of $\Gamma_3$ with eigenvalues $\pm1/2$. In reality the vortex profile is not infinitely smooth and a scattering between two valleys $\mathbf{K}_{+}$ and $\mathbf{K}_{-}$ exists. This introduces a pseudospin SU(2) breaking perturbation to the zero modes. Within the subspace spanned by Eq. (2) such perturbation is described by $-\boldsymbol{B}_{\mathrm{eff}}\cdot\Gamma$. With $\boldsymbol{B}_{\mathrm{eff}}\neq0$ the only conserved pseudospin quantum number is the component of pseudospin along the direction of $\boldsymbol{B}_{\mathrm{eff}}$.

With the pseudospin SU(2) symmetry breaking the SC vortex core acquires interesting textures which allows experimental detection. As we shall discuss below, this texture is in the form of site or bond CDW. The site CDW breaks the equivalence between the $A$ and $B$ sublattice without enlarging the unit cell. It is described by a real order parameter. On the other hand the bond density wave (or Kekule order[11]) triples the unit-cell size and is described by two real order parameters each corresponding to one of the two complementary Kekule distortion patterns.[11] Each of these order parameters can be described in the Dirac Hamiltonian $K$ as a mass term (or fermion bilinear) $\int d\mathbf{r}\Psi^{\dagger}\phi_aM_a\Psi$ where $M_a$ is the mass matrix representing an order (Table I) and $\phi_a$ the amplitude of the corresponding order parameter. When pro-

TABLE I. The five mass matrices associated with the Kekule, CDW, and the SC order parameters.

| Order parameter type | Mass matrix |
|---|---|
| Kekule 1 | $M_1=\sigma_x\tau_y\rho_0$ |
| Kekule 2 | $M_2=\sigma_y\tau_y\rho_z$ |
| CDW | $M_3=\sigma_0\tau_z\rho_z$ |
| Real SC | $M_4=\sigma_x\tau_z\rho_x$ |
| Imaginary SC | $M_5=\sigma_x\tau_z\rho_y$ |

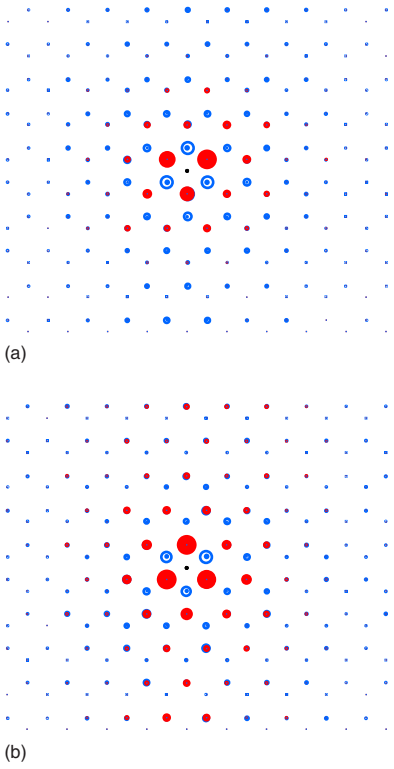


FIG. 3. (Color online) CDW texture of the vortex core states for (a) positive and (b) negative energy in the presence of a small staggered chemical potential around the core. Whorled (blue)/filled (red) dots show surplus/deficit quasiparticle density, with their size proportional to the magnitude.

jected on to the two-dimensional space of the midgap states, $M_{1,2,3} \equiv \Gamma_{1,2,2}$, and the three order parameters (site CDW and two Kekule distortions) correspond to the $z,x,y$-component of $\boldsymbol{B}_{\text{eff}}$, respectively.

We have studied two different types of pseudospin SU(2) breaking by solving the BdG Hamiltonian numerically on a finite graphene lattice. In the first case, we take a graphene lattice with edges at zero staggered chemical potential (Fig. 2), in which case the induced SU(2) symmetry-breaking term $\boldsymbol{B}_{\text{eff}}$ turns out to point primarily in the $x$-$y$ plane leading to a Kekule type vortex texture. In Fig. 2 we plot the expectation value of the nearest-neighbor link operator $c_{is}^{\dagger}c_{js}$ in the core states ($c_{is}^{\dagger}$ is the lattice electron operator at $i$-th site with spin $s$). Here dotted blue (solid red) bonds denote the positive (negative) expectation value $\langle c_{is}^{\dagger}c_{js}\rangle > 0$ ($<0$) and the thickness represents the amplitude ($|\langle c_{is}^{\dagger}c_{js}\rangle|$). It is interesting to note that the Kekule texture associated with the two split core states are opposite.

The second type of pseudospin symmetry breaking is triggered by explicitly turning on a staggered chemical potential. This can be achieved through the interaction with the "buffer layer" when graphene is grown on a substrate[12] [Fig. 1(b)]. In Figs. 3(a) and 3(b) we show the induced site CDW texture associated with the two core states. Similar to the Kekule texture discussed above, the site CDW texture associated with the two core states are complementary. In principle these vortex core texture can be probed by scanning tunneling microscope (STM). In addition, the two core states carrying the opposite $Q_3$ charge can also be detected by measuring their orbital magnetic moment: As shown in Ref. 13, a graphene quasiparticle carrying a $Q_3$ quantum number has, in the presence of staggered chemical potential, a finite orbital magnetic moment with the opposite direction for each valley.[13] The complimentary nature of the texture of the two modes is important for differentiating the effect we are studying from any other such effect generated simply by translation symmetry breaking. Also notice that changing the direction of magnetic field in the vortex core simply changes the pattern to its complimentary one, which is another unique feature of our results.

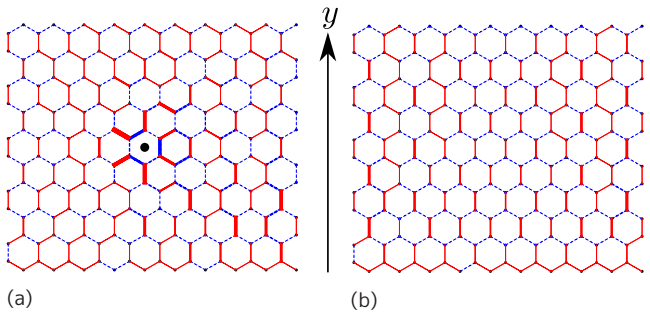


FIG. 4. (Color online) The Kekule texture in the presence of supercurrent $J$ in $y$-direction. The relative amplitude $\Sigma_s\langle c_{is}^{\dagger}c_{js}+\text{H.c.}\rangle_{J\neq 0}-\Sigma_s\langle c_{is}^{\dagger}c_{js}+\text{H.c.}\rangle_{J=0}$, where $\langle\cdots\rangle_{J\neq 0}$ ($\langle\cdots\rangle_{J=0}$) is the expectation value in the presence (absence) of supercurrent $J$, is plotted for each nearest-neighbor bond where dotted (blue)/solid (red) lines show strengthened/weakened bonds, respectively: (a) with a vortex located at the position of the black dot and (b) without vortices.

In Fig. 4(a), we demonstrate another effect—the QVHE. A single vortex is created at the center of the central SC graphene region and a finite supercurrent $J$ is passed along the strip by spatially twisting the phase of SC order parameter. Interestingly the Kekule type pattern in Fig. 2 is shifted in the direction perpendicular to the supercurrent, manifesting the accumulation of the pseudospin moment (recall that this is the component of pseudospin in the $\boldsymbol{B}_{\text{eff}}$ direction).

Although the accumulation of pseudospin by supercurrent can be viewed as a close relative of the QSHE, unlike the spin-filtered gapless mode at the quantum spin Hall (QSH) edge, generically there is no gapless edge mode in the QVHE. This is because in the QSH edge, it is the time-reversal symmetry that protects the gapless edge modes. There is no such discrete symmetry for the pseudospin that can protect the gapless edge state in the QVHE. In other word, quite generally, the edge mode of the QVHE is gapped because of pseudospin SU(2) symmetry breaking, leading to the Kekule or CDW texture at the edge. This is reminiscent to the QSHE where an electric field can induce spin accumulation.

The QVHE was proposed previously for graphene with staggered chemical potential[14] and for biased bilayer graphene,[15] where the pseudospin symmetry is broken in the bulk in $z$-direction, and of interest there was $z$-component of pseudospin current. On the other hand, in our setup, SU(2) pseudo spin symmetry is not broken by bulk SC order parameter, while symmetry breaking can take place near the

sample boundary or a defect, in arbitrary direction.

Like the QSHE the above phenomena (pseudospin 1/2 vortex core and the QVHE) can be summarized by a "double Chern-Simons" action,

$$S_{\mathrm{CS}}[A,A^5,\Phi]=\frac{\pm 1}{2\pi}\int dtd\mathbf{r}\varepsilon^{\mu\nu\rho}A^5_\mu\partial_\nu(\bar{\Phi}\partial_\rho\Phi-2A_\rho) \quad (3)$$

where $A_\mu$ and $A^5_\mu$ are the external (source) gauge fields that minimally couple to the electromagnetic current and to the current of the conserved component of pseudospin, respectively, and $\Phi=e^{i\phi}$ is the phase factor of the superconducting order parameter. [In writing down Eq. (3) we have absorbed the electronic charge into the definition of $A$ so that the flux quantum is $2\pi$.] The sign in Eq. (3) is determined by the pseudospin quantum number of the in-gap level that lies below the Fermi energy. Formally $S_{\mathrm{CS}}$ can be derived by integrating out the gapped fermionic quasiparticles following the method introduced in Ref. 16. Due to space limitation, we cannot include the details of such derivation. Instead, we will just show that the predictions from the effective action are consistent with the earlier numerical results. By differentiating $S_{\mathrm{CS}}$ with respect to $A^5_\mu$ we obtain $J^5_\mu=\pm(1/2\pi)\epsilon^{\mu\nu\rho}\partial_\nu(\bar{\Phi}\partial_\rho\Phi-2A_\rho)$. Recalling that $(1/2\pi)\epsilon^{\mu\nu\rho}\partial_\nu\bar{\Phi}\partial_\rho\Phi$ is the $\mu$th component of the vortex current, we immediately see, from the $\mu=0$-th component of the above result, that the vortices carry pseudospin discussed in Figs. 2 and 3. Similarly, a time-dependent supercurrent $\partial_0\bar{\Phi}\partial_k\Phi\neq 0$ gives rises to a pseudospin current $\epsilon^{kj}J^5_j$. Thus ramping the supercurrent from zero to some fixed value will result in an accumulation of the pseudospin as shown in Fig. 4.

Double Chern-Simons action (3) predicts pseudospin accumulation by supercurrent even without any vortices: In Fig. 4(b) we plot the expectation value of the bond operator in the absence of vortices. Clearly a bond density wave is induced by the supercurrent. The presence of the vortices in Fig. 4(a) just enhances the effect. Although the supercurrent induces the Kekule pattern without vortices the latter is not energetically close to be realized. In fact none of the orders we discuss above are low energy, near condensing, modes of graphene (recall that superconductivity is induced externally). Likewise the fact that superconducting vortices exhibit the Kekule/CDW pattern is not due to the usual Ginzburg-Landau mechanism where the suppression of an order enhances its competing order. Rather it is due to a quantum duality encapsulated by the Wess-Zumino-Witten (WZW) physics we discuss in the following.

The fact that a topological defect in one order parameter carries a quantum number of another order parameter is dictated by the WZW term[17] in the quantum action of competing order parameters. Indeed when several nearly degenerate order parameters compete to open mass gaps in a massless Dirac theory, one can derive a nonlinear sigma model to describe the low energy/long-wavelength order-parameter fluctuations by integrating out the fermion fields. When the "mass term" associated with these orders obey certain anticommutation relation, a purely topological term, the WZW term, arises. For example, the five order parameters we have encountered, namely, the real and imaginary parts of SC order parameter, two Kekule and one CDW order parameters, give rise to five mass-generating fermion bilinear $\int d\mathbf{r}\Sigma_{a=1}^5\Psi^\dagger\phi_a M_a\Psi$ in graphene. The five Hermitian mass matrices $M_a$ anticommute with each other, $\{M_a,M_b\}=2\delta_{ab}$, $(a,b=1,\ldots,5)$, and also with the kinetic term, $\sigma_0\tau_x\rho_0 p_x+\sigma_z\tau_y\rho_z p_y$, of graphene. The five mass matrices are given in Table I. The WZW term generated upon integrating out the fermion fields[16] is $S_{\mathrm{WZW}}=-(3i/4\pi)\epsilon^{abcde}\int_0^1 du\int d^3x\phi_a\partial_u\phi_b\partial_\tau\phi_c\partial_x\phi_d\partial_y\phi_e$. As discussed by Abanov and Wiegmann[16] this term encodes soliton (defect) quantum number, their mutual statistics, etc. What is perhaps less appreciated is the fact that the physics of the WZW term is manifested even when the order parameters in question are not low energy degrees of freedom as it is the case here. Thus the WZW term is at the heart of both the QVHE and the deconfined quantum criticality.

In summary we have shown that the quantum duality dictated by the WZW term implies a SC vortex core with Kekule or CDW order-parameter texture as well as the QVHE in proximity-induced SC graphene. Experimental consequences are predicted.

D.H.L. was supported by DOE Grant No. DE-AC02-05CH11231. P.G. acknowledges support from LBNL DOE Grant No. 504108. S.R. thanks the Center for Condensed Matter Theory at University of California, Berkeley for its support.

[1] K. S. Novoselov *et al.*, Science **306**, 666 (2004).
[2] K. S. Novoselov *et al.*, Nature (London) **438**, 197 (2005).
[3] H. B. Heersche *et al.*, Nature (London) **446**, 56 (2007).
[4] A. Shailos *et al.*, EPL **79**, 57008 (2007).
[5] C. W. J. Beenakker, Phys. Rev. Lett. **97**, 067007 (2006).
[6] P. Ghaemi and F. Wilczek, arXiv:0709.2626 (unpublished).
[7] C. L. Kane and E. J. Mele, Phys. Rev. Lett. **95**, 226801 (2005).
[8] B. Bernevig *et al.*, Science **314**, 1757 (2006).
[9] T. Senthil *et al.*, Science **303**, 1490 (2004).
[10] D. L. Bergman and K. Le Hur, Phys. Rev. B **79**, 184520 (2009).
[11] C.-Y. Hou, C. Chamon, and C. Mudry, Phys. Rev. Lett. **98**, 186809 (2007).
[12] S. Y. Zhou *et al.*, Nature Mater. **6**, 770 (2007).
[13] D. Xiao, W. Yao, and Q. Niu, Phys. Rev. Lett. **99**, 236809 (2007).
[14] G. W. Semenoff, Phys. Rev. Lett. **53**, 2449 (1984).
[15] I. Martin, Ya. M. Blanter, and A. F. Morpurgo, Phys. Rev. Lett. **100**, 036804 (2008).
[16] A. G. Abanov and P. B. Wiegmann, Nucl. Phys. B **570**, 685 (2000).
[17] A. Tanaka and X. Hu, Phys. Rev. Lett. **95**, 036402 (2005).